# Probing Decoherence through Fano Resonances

Andreas Bärnthaler, Stefan Rotter,* Florian Libisch, and Joachim Burgdörfer
*Institute for Theoretical Physics, Vienna University of Technology, A–1040 Vienna, Austria, EU*

Stefan Gehler, Ulrich Kuhl, and Hans-Jürgen Stöckmann
*Fachbereich Physik, Philipps-Universität Marburg, Renthof 5, D-35032 Marburg, Germany, EU*

(Received 19 January 2010; published 26 July 2010)

We investigate the effect of decoherence on Fano resonances in wave transmission through resonant scattering structures. We show that the Fano asymmetry parameter $q$ follows, as a function of the strength of decoherence, trajectories in the complex plane that reveal detailed information on the underlying decoherence process. Dissipation and unitary dephasing give rise to manifestly different trajectories. Our predictions are successfully tested against microwave experiments using metal cavities with different absorption coefficients and against previously published data on transport through quantum dots. These results open up new possibilities for studying the effect of decoherence in a wide array of physical systems where Fano resonances are present.

DOI: 10.1103/PhysRevLett.105.056801 PACS numbers: 73.23.−b, 03.65.Yz, 05.45.Mt, 42.25.Bs

One of the central issues of current research in quantum mechanics is *decoherence* [1], i.e., the loss of coherence induced in a system by the interaction with its environment. Studying the ubiquitous effects of decoherence is not only of fundamental interest for the understanding of the quantum-to-classical crossover, but is the key to the realization of operating quantum information devices which rely on long coherence times [2,3]. To this end, decohering processes need to be controlled and suppressed. In practice, however, enumeration and identification of sources of decoherence is already a challenging task on its own (see, e.g., [4,5]). This is, in part, due to the fact that different decoherence channels are difficult to distinguish from one another since their influence on the observables of interest is often very similar.

Decoherence in quantum systems is, typically, described within the framework of an open quantum system approach by a quantum master equation of, e.g., the Lindblad form [6]. In this framework, the reduced density operator, $\rho$, of the open system with Hamiltonian $H_S$ interacting with the environment through Lindblad operators $L_j$ evolves as,

$$i\dot{\rho} = [H_S, \rho] + i\Big[\sum_j L_j \rho L_j^\dagger - \tfrac{1}{2}(L_j^\dagger L_j \rho + \rho L_j^\dagger L_j)\Big]. \quad (1)$$

The system-environment interactions allow for a decohering, yet unitary evolution of the system within the Markov approximation. In the special case that only the last term of the coupling in Eq. (1) ($\sim L_j^\dagger L_j \rho + \rho L_j^\dagger L_j$) is present, interaction with the environment is purely dissipative. The counterterm $\sim L_j \rho L_j^\dagger$ acts as source and preserves the unitarity of the evolution. Characterizing the system-environment interaction for a given physical realization is one of the major challenges of decoherence theory. In this Letter, we show that Fano resonances, specifically the asymmetry parameter $q$, allows us to disentangle different decoherence mechanisms present in resonant scattering devices such as quantum dots [5,7–10] (for a review see [11]). The $q$ parameter follows, as a function of the decoherence strength, trajectories in the complex plane that are specific to the underlying environmental coupling. In particular, dissipation and decoherent dephasing can be distinguished from each other.

Fano line shapes in transport result from the interference between different channels in the transmission amplitude [12],

$$t(k) = z_r \frac{\Gamma/2}{k - k_{\mathrm{res}} + i\Gamma/2} + t_d, \quad (2)$$

with $t_d$ the amplitude of a (smoothly varying) direct (or background) channel and $z_r$ the strength, $k_{\mathrm{res}}$ the position, and $\Gamma$ the width of the resonant channel. The transmission probability in the vicinity of the resonance, $|t(k)|^2$ takes on the form of a Fano profile,

$$|t(k)|^2 = |t_d|^2 \frac{|\varepsilon + q|^2}{1 + \varepsilon^2}, \quad (3)$$

in terms of the reduced wave number (or energy) $\varepsilon = (k - k_{\mathrm{res}})/(\Gamma/2)$. The asymmetry parameter $q$ determines the shape of the Fano resonance. In the limit $q \to \pm\infty$, the symmetric Breit-Wigner shape is recovered while for $q \to 0$ window (or "anti-") resonances appear. For single-channel scattering through systems with time-reversal symmetry (TRS) $q$ is strictly real [13,14]. When TRS is broken, Eq. (3) still holds, but $q$ may take on complex values [15]. The generalization of the Fano $q$ parameter is therefore ideally suited as a sensitive probe of TRS-breaking processes. An Aharonov-Bohm ring exposed to a TRS-breaking magnetic field was recently shown to exhibit $q$ parameters performing periodic oscillations in

 

the complex plane [8]. Decoherence, being a prime example for breaking TRS, should leave distinct signatures in the behavior of $q$ as well [8–10,15–17]. In the present Letter, we provide experimental and theoretical evidence that the complex $q$ trajectory reveals details on the underlying decoherence process that are characteristically different for dissipation and irreversible dephasing.

We first consider ballistic transport through a scattering cavity in the presence of uniform dissipation, the strength of which is independent of the wavelength or position inside the cavity [Fig. 1(a)]. For the corresponding open quantum system this corresponds to the reduction of the coupling to the environment [Eq. (1)] to sink terms $(\sim L_j^\dagger L_j \rho + \rho L_j^\dagger L_j)$ only. Physical realizations of pure dissipation in quantum dots include electron-hole recombination and currents leaking into the substrate. For classical wave scattering [18] the presence of dissipation in a resonant device shifts the resonance positions $k_{\mathrm{res}} \rightarrow \bar{k}_{\mathrm{res}} = k_{\mathrm{res}} - \Delta k - i\kappa$. Since, in relative terms, the broadening of the resonance width $\kappa$ usually dominates over $\Delta k$, Eq. (2) is modified as follows:

$$t(k) \approx z_r \frac{\Gamma/2}{k - k_{\mathrm{res}} + i\Gamma/2 + i\kappa} + t_d, \tag{4}$$

with a broadened resonance width $(\Gamma + 2\kappa)$.

As convenient measure for the strength of decoherence, we use the ratio $\chi = 2\kappa/(\Gamma + 2\kappa)$, with the limiting cases $\chi = 0$ in the absence of decoherence and $\chi = 1$ for dissipation-dominated broadening. With Eq. (4) the generalized $q$ parameter in Eq. (3) now becomes,

$$q(\chi) = q_0 + \chi(i - q_0), \tag{5}$$

where $q_0$ is the real $q$ parameter in the absence of dissipation. For increasing dissipation strength, the complex Fano

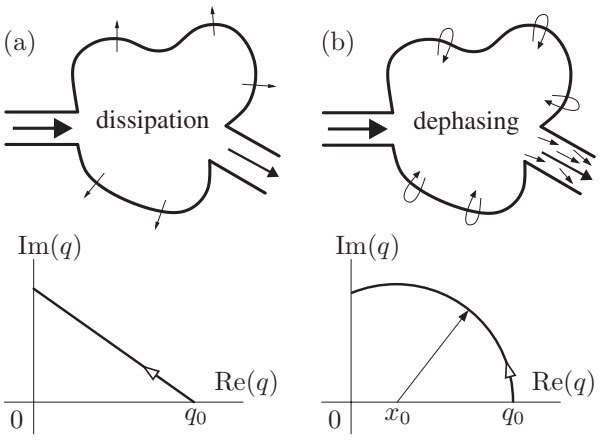


FIG. 1. Dependence of the complex Fano asymmetry parameter $q$ on the decoherence strength $\chi$. In the case of a uniformly dissipative system (a), an increase of $\chi$ shifts $q(\chi)$ in the complex plane along a *straight line* away from a real value $q_0$; while for a uniformly dephasing system (b), the trajectory $q(\chi)$ forms a *circular arc*. This arc is centered at $x_0$ on the real axis, thus featuring a vertical tangent at $q_0$.

$q$ parameter follows a straight-line trajectory in the complex plane [see Fig. 1(a)] which, for large dissipation strength ($\chi \rightarrow 1$), approaches the limit $q = i$. The linear form of $q(\chi)$ follows from the assumption entering Eq. (4) that only the resonant but not the direct amplitude ($t_d$) is affected by decoherence—an assumption which generally holds well for resonant scattering devices (including microwave cavities).

The analytical dependence of $q$ on the decoherence strength has previously been studied in the case of dephasing [Fig. 1(b)] as the main source of decoherence [15]. Here, in contrast to the dissipative case, the flux in the system is conserved even at finite coherence lengths. A simple realization of flux-conserving decoherent dephasing for ballistic transport is given by the Büttiker dephasing probe [19]: By attaching a fictitious voltage probe, the coherent scattering paths from source to drain are accompanied by incoherent paths via the voltage probe which randomizes the phase information. To convert the dissipative voltage probe into a flux-conserving dephasing probe, the potential of the probe is chosen such that the flux leaving through the probe is incoherently injected back into the cavity. This corresponds to the presence of both sink and source terms in the Liouvillian operator [Eq. (1)] with an infinite number ($j = 1, \ldots, \infty$) of coupling terms with random phases. Such an incoherent reinjection of flux is fully accounted for by an additional Breit-Wigner shaped term in the Fano profile,

$$|t(k)|^2 = |t_d|^2 \left[ \frac{\{\varepsilon' + \mathrm{Re}[q(\chi)]\}^2}{1 + \varepsilon'^2} + \frac{\mathrm{Im}[q(\chi)]^2}{1 + \varepsilon'^2} \right], \tag{6}$$

with the reduced wave number now rescaled to the increased resonance width $\varepsilon' = (k - k_{\mathrm{res}})/(\Gamma/2 + \kappa)$ as well as $\mathrm{Re}[q(\chi)] = q_0(1 - \chi)$ and $\mathrm{Im}[q(\chi)]^2 = \chi[1 + q_0^2(1 - \chi)]$. By eliminating $\chi$ from these expressions, one finds

$$\{\mathrm{Re}[q(\chi)] - x_0\}^2 + \mathrm{Im}[q(\chi)]^2 = r_0^2, \tag{7}$$

where $x_0 = [q_0 - 1/q_0]/2$ and $r_0^2 = 1 + x_0^2$ are independent of $\chi$. Thus $q(\chi)$ describes a circle in the complex plane centered at $(x_0, 0)$ on the real axis and converging to $q(\chi \rightarrow 1) = i$ [see Fig. 1(b)]. We find circular trajectories in the complex $q$ plane also for a different (more general) scenario of dephasing modeled by gradually suppressing the interference term between the direct and the resonant transmission in Eq. (2) as $\chi \rightarrow 1$ (for details see [20]). Also here the circle is centered on the real axis, but imaginary values for $q(\chi \rightarrow 1)$ may differ from $i$.

We conclude that for the same Fano resonance as determined by the $q(\chi \rightarrow 0) = q_0$ limit, the complex generalization of $q$ evolves along different trajectories for finite $\chi$ for purely dissipative (on a straight line) and dephasing (on a circular arc) decoherence. Even for small $\chi$ where $q$ is close to the real axis characteristic differences appear: the dephasing trajectory has a tangent parallel to the imaginary axis while the dissipative trajectory takes off at an angle

arctan$(1/q_0)$ relative to the $x$ axis. This finding suggests that by following the $q(\chi)$ trajectory for a given Fano resonance, the underlying decoherence process can be unambiguously identified.

An ideal system for the controlled experimental verification of the above theoretical results are microwave cavities which have been successfully employed in the past as analog simulators of a wide variety of quantum transport phenomena [21]. As was shown recently, well-separated Fano resonances can be measured with high accuracy in such systems [17]. The transport of microwaves into and out of the cavity can be controlled via shutters at both ends, which in turn determine the $q_0$ values of resonances. Because of the finite conductivity of the cavity and the resulting dissipation of flux in the cavity walls, decoherence is naturally present. Furthermore, we can control the degree of dissipation by cooling the cavities to lower temperatures or by fabricating cavities with identical geometry out of different materials. To a good degree of approximation, the power loss can be assumed to be uniform and mode-independent [as in Eq. (4)].

For the experiment we used rectangular microwave cavities (length $L = 176$ mm, width $D = 39$ mm) [see Fig. 2(a)] made out of copper, brass, and steel with different conductivities $\sigma$ [at room temperature: $\sigma = 54.22\ \mathrm{m}/(\Omega\,\mathrm{mm}^2)$ for copper, $\sigma = 12.20\ \mathrm{m}/(\Omega\,\mathrm{mm}^2)$ for brass, and $\sigma = 1.37\ \mathrm{m}/(\Omega\,\mathrm{mm}^2)$ for steel]. The cavities were terminated by two metallic shutters each with opening width $s = 8.8$ mm and a thickness of 1 mm. Two aluminum leads with length $l = 200$ mm and width $d = 15.8$ mm were attached to the openings. The measurements were carried out using a microwave vector analyzer connected via coaxial cables and adapters at the end of each lead. We note that the measuring device is thus "part of the semi-infinite lead" and not an additional measurement channel [5]. Measurements were performed in the frequency range with exactly one transverse mode in each lead thus coupling to the first and third transverse modes of the cavity (see Ref. [17] for details).

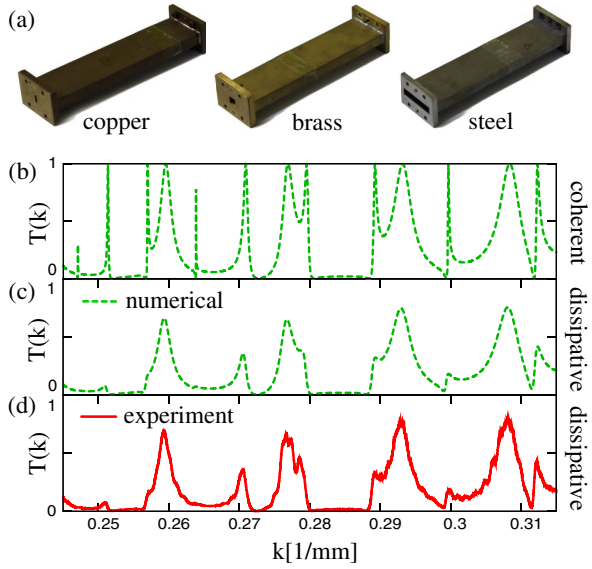


FIG. 2 (color online). (a) Rectangular microwave cavities of identical dimensions, but out of different materials. The left two cavities are shown with a shutter at the opening as used for tuning the Fano parameter. (b)–(d) Wave number dependence of transmission $T(k)$ through a cavity. In (b) the fully coherent limit is shown. Panels (c) and (d) display the transmission with the dissipative decoherence as present in the steel cavity at room temperature. Theoretical MRGM (c) and experimental data (d) show excellent agreement on an absolute scale.

The experimental transmission data $T(k) = |t(k)|^2$ recorded for the steel cavity display well-separated Fano resonances [see Fig. 2(d)]. For comparison we also show the corresponding numerical results including dissipation [see Fig. 2(c)] and without dissipation [see Fig. 2(b)]. The numerical data were obtained with the modular recursive Green's function method (MRGM) [22], where uniform microwave attenuation by dissipation following [18] was taken into account. Even though the effect of dissipation is quite sizeable, we find excellent agreement between theory and experiment [see Figs. 2(c) and 2(d)]. The small oscillations in the experimental data not reproduced by the numerical calculations can be attributed to standing waves induced by the minimal reflection from the adapters (less than 1%). The influence on the Fano resonances is, however, negligible as compared to the dominant decoherence process, i.e., the Ohmic losses in the cavity walls. Accordingly, Eq. (5) predicts the $q$ parameters of Fano resonances to display linear decoherence trajectories in the complex plane. To verify this prediction, we now extract the complex Fano $q$ parameter from resonances at different decoherence strengths as determined by the different cavity materials and their temperature dependence (on each cavity one measurement was performed at ambient temperature and at liquid nitrogen cooling). Since the Fano resonance formulas Eqs. (2) and (3) are strictly only valid for a direct amplitude $t_d$ which is $k$ independent, we exclude resonances from our analysis for which this requirement is not satisfied. For resonances satisfying this requirement we extract the $q$ parameters by selecting the minimum, maximum, and one intermediate value as fitting points in the experimental transmission probabilities [as, e.g., in Fig. 2(d)]. Following each resonance for different degrees of dissipation thus allows us to obtain the desired decoherence trajectories in the complex $q$ plane. To facilitate the comparison of the behavior of different members of the ensemble of resonances we rescale all data $[q \to \tilde{q} = \mathrm{Re}(q)q_0^{-1} + i\mathrm{Im}(q)]$ onto a single "universal" trajectory which connects the points $\tilde{q} = 1$ and $\tilde{q} = i$. The data shown in Fig. 3(a) demonstrates that the expected linear behavior is, indeed, observed.

Such a linear trajectory due to pure dissipation can now be contrasted with the circular trajectory for flux-conserving dephasing. For open quantum systems this corresponds to the presence of an infinite number of source

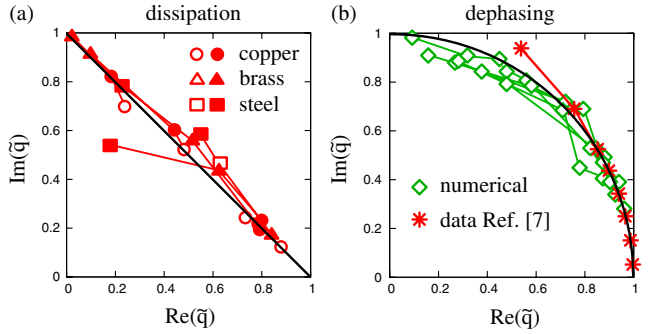


FIG. 3 (color online). (a) Complex Fano $q$ parameter extracted from microwave experiments on copper, brass, and steel cavities. For each material, measurements were performed at room temperature (filled symbols) and liquid nitrogen temperature (open symbols). (b) Fano parameter corresponding to the theoretical MRGM data for a dephasing cavity (diamond) and the experimental data from Ref. [7] (asterisk). Data points for the same resonance at different decoherence strengths are connected by lines and rescaled, $q \rightarrow \tilde{q}$, to reach $\tilde{q} = 1$ ($\tilde{q} = i$) in the fully coherent (incoherent) limit. The straight (circular) black curve in (a) [(b)] displays the theoretical prediction following Eq. (5) [Eq. (7)] for the case of uniform dissipation (dephasing).

($\sim L_j \rho L_j^\dagger$) and sink terms ($\sim L_j^\dagger L_j \rho + \rho L_j^\dagger L_j$) in Eq. (1) as induced, e.g., by wave number independent electron-phonon coupling. In the classical electromagnetic cavity such a flux-restoring incoherent source is difficult to realize. However, in our simulation we can numerically reinject the dissipated power into the rectangular cavity, leaving the scattering system otherwise unchanged. The dissipated flux to be symmetrically reinjected is determined as the difference between transmission plus reflection and the unitary limit, $1 - |t(k)|^2 - |r(k)|^2$. The $q$ values extracted from the numerically determined Fano profiles are also mapped onto a universal circular arc with radius 1 centered at $x_0 = 0$. The data obtained for several Fano resonances closely follow the circular trajectory [Fig. 3(b)] confirming the dependence of the $q(\chi)$ trajectory on the underlying decoherence mechanism.

To also test our predictions for a true quantum scattering system, we reanalyzed published experimental data on Fano resonances in transport through resonant quantum dots [7]. For these conductance measurements in the temperature range 100 mK $\leq T \leq$ 800 mK, we find the evolution of $q(T)$ in the complex plane to be very well described by a circular arc [see Fig. 3(b)]—as predicted for flux-preserving dephasing. Details of this analysis as well as a comparison between the experimental and the theoretical Fano resonance curves are provided in [20].

In conclusion, we have demonstrated that Fano resonances may serve as sensitive probes of decoherence in wave transport. We find that for increasing dephasing or dissipation strength the Fano asymmetry parameter $q$ evolves on circular arcs or on straight lines in the complex plane. As confirmed by measurements on microwave cavities and on quantum dots, these characteristic signatures provide a means to determine not only the degree but also the specific type of decoherence present in the experiment. It is hoped that the present findings will stimulate future experimental investigations of the influence of decoherence on the Fano $q$ parameter in resonant quantum transport.

We thank K. Kobayashi for very helpful discussions and the Austrian FWF (P17359 and SFB016) as well as the German DFG (FOR760) for support.

*Corresponding author: stefan.rotter@tuwien.ac.at

[1] W. H. Zurek, Rev. Mod. Phys. **75**, 715 (2003).
[2] D. Bouwmeester, A. Ekert, and A. Zeilinger, *The Physics of Quantum Information* (Springer, New York, 2000).
[3] J. J. Lin and J. P. Bird, J. Phys. Condens. Matter **14**, R501 (2002).
[4] R. Simmonds *et al.*, Phys. Rev. Lett. **93**, 077003 (2004).
[5] B. Elattari and S. A. Gurvitz, Phys. Rev. Lett. **84**, 2047 (2000); J. Z. Bernád, A. Bodor, T. Geszti, and L. Diósi, Phys. Rev. B **77**, 073311 (2008).
[6] G. Lindblad, Commun. Math. Phys. **48**, 119 (1976).
[7] I. G. Zacharia *et al.*, Phys. Rev. B **64**, 155311 (2001).
[8] K. Kobayashi, H. Aikawa, S. Katsumoto, and Y. Iye, Phys. Rev. Lett. **88**, 256806 (2002); Phys. Rev. B **68**, 235304 (2003).
[9] A. C. Johnson, C. M. Marcus, M. P. Hanson, and A. C. Gossard, Phys. Rev. Lett. **93**, 106803 (2004).
[10] W. Gong, Y. Zheng, J. Wang, and T. Lü, Phys. Status Solidi B **245**, 1175 (2008).
[11] A. E. Miroshnichenko, S. Flach, and Y. S. Kivshar, arXiv:0902.3014.
[12] U. Fano, Phys. Rev. **124**, 1866 (1961).
[13] Note that the $q$ parameter is complex for multichannel scattering with TRS [14] (a case not considered here).
[14] M. Mendoza *et al.*, Phys. Rev. B **77**, 155307 (2008).
[15] A. A. Clerk, X. Waintal, and P. W. Brouwer, Phys. Rev. Lett. **86**, 4636 (2001).
[16] Z. Zhang and V. Chandrasekhar, Phys. Rev. B **73**, 075421 (2006).
[17] S. Rotter *et al.*, Phys. Rev. E **69**, 046208 (2004); Physica E (Amsterdam) **29**, 325 (2005).
[18] J. D. Jackson, *Classical Electrodynamics* (Wiley, New York, 1998).
[19] M. Büttiker, Phys. Rev. B **33**, 3020 (1986); IBM J. Res. Dev. **32**, 63 (1988).
[20] See supplementary material at http://link.aps.org/supplemental/10.1103/PhysRevLett.105.056801 for an explicit derivation of the form of complex $q$ trajectories in the case of dephasing and for details on the employed fitting procedures.
[21] H. J. Stöckmann, *Quantum Chaos: An Introduction* (Cambridge University Press, Cambridge, 1999).
[22] S. Rotter *et al.*, Phys. Rev. B **62**, 1950 (2000); **68**, 165302 (2003).